

Ultrasonic studies of n-Ge sample by buffer-rod

P. PETCULESCU*

Department of Physics, Ovidius University of Constanta, 900527, Romania

In this paper, we used a nondestructive method with ultrasounds to measure acoustic and spectral parameters for two Ge samples, one doped with As and another one pure. We examined the variation of the ultrasound attenuation and velocity, under the influence of temperature and frequency which characterize the mechanical properties of the semiconductor sample material, such as elastic constants C_{ij} , transversal modules G_{111} and G_{100} , the anisotropy factor A and the nonlinearity parameter β . We give one empirical relation vs. the adiabatic approximation for the elastic constants. Our results are in agreement with the modern theory of crystal lattices elaborated by Leibfried and Ludwig, which give a general relationship between the elastic constants and the temperature considering the anharmonic nature of the atomic oscillations. Measurements were made using two successive echoes and for each measurement point, the saved information consists of the amplitude and velocity determined from the reflected RF signal by the USIS program. We used the temperature range from 273 K to 873 K and the frequency domain from 2 MHz to 20 MHz, using Nortec and Krautkramer transducers. Probing at high temperatures was made possible using an Al buffer-rod interposed between the transducer and the sample. The experimental measurements were made using an ultrasonic device Sonic 136 Ultra made by Staveley Corporation.

(Received February 14, 2006; accepted July 20, 2006)

Keywords: Semiconductors, Ultrasounds, Elastic constants, Attenuation, Buffer-rod

1. Introduction

Characterization of material microstructure, which includes the determination of dislocations, anisotropy factor, elastic modulus, cracks and nonlinearity parameter, plays an important role in ensuring the quality of the estimation of mechanical properties and the determination of the amount and rate of structures and components degradation [1]. An important interest exists concerning the effects of mechanical stresses resulting from the crystal growth and the device processing on the behavior and reliability of semiconductor devices; the deposition of various layers introduces stresses in semiconductors having maximum magnitudes at the film-semiconductor interface. Experimentally, strains have been determined directly in some cases, but precise computation of the stresses requires knowledge of elastic modulus, nonlinearity parameter, ultrasonic attenuation vs. temperature and frequency for specific orientations within the crystallographic plane defining the surface of the semiconductor.

Taking into consideration that the elastic medium is a semiconductor, the increase of the ultrasonic attenuation might be due to the increase of the density of free electrons. Generally, the ultrasonic attenuation or the loss of the acoustic energy is due to the apparent losses and physical losses, respectively. In the case of apparent losses, the losses by diffraction have an important role, while the physical losses are due mainly to the dislocations and to the contribution of free electrons (absorption and scattering phenomena). The elimination of losses by diffraction from the total losses determined experimentally led to the finding of the physical losses, and in the case of

ultrasounds, to the determination of the intrinsic attenuation.

The attenuation and the corresponding transfer function are monoton functions of frequency, but due to some 'variations' such as limited bandwidth and noise influence, the functions determined experimentally possess an oscillating character. Therefore, it is better practically to use an attenuation approximation which depends on frequency, presented in an analytic form. This is why, many laws of approximation of attenuation can be used. For semiconductors, the best results are obtained by using an approximation of the power law. In this case, the attenuation depending on frequency can be expressed in dB by $\alpha(f) = Af^n$, where the coefficients A and n are defined by the material properties.

2. Experimental

2.1 Theory

2.1.1 Elastic constants and the adiabatic approximation

For this purpose it is necessary to experimentally determine the longitudinal and shear ultrasound velocities in the sample. By pulse-echo method, the elastic constants of a solid sample can be determined. The sample subjected to the experiments that is Ge semiconductor, bears three elastic constants corresponding to the cubical system [2]. One can easily notice that C_{11} and C_{44} can be obtained in a more direct manner from the longitudinal and shear velocities data, while C_{12} can be obtained only indirectly.

Given the fact that the actual experimental conditions do not generally follow these requirements there are errors

between the transducer and the examined sample, due to the following causes :

- the misalignment between the crystal orientation and the required crystallographic axis;
- the diffraction that appears because the transducer has a finite diameter and the acoustic pressure received in different points do not have the same phase;
- the fact that in the near field, the presence of the lateral surfaces limiting the propagation medium influences the oscillation mode and the propagation velocity becomes dependent on the lateral size of the sample and the wavelength.

In the adiabatic approximation we assumed zero change in the thermal energy during the successive contraction-dilatation processes which occur while ultrasonic waves propagate through the material. In ambient temperature conditions, the elastic constants are influenced by the energy of the atomic oscillations, which are assumed to have the following temperature dependence [3] :

$$C_{ij}(T) = C_{ij}^0 (A - BT) \quad (1)$$

where C_{ij}^0 are the elastic constants corresponding to 0 K. Making allowances for the fact that the contraction-dilatation process and the temperature variation of the elastic constants are included by the anharmonic nature of atomic oscillations, a more general model can be applied:

$$C_{ij}(T) = C_{ij}^0 [1 - D_{ij}E(T)] \quad (2)$$

where D_{ij} – are the anharmonic coefficients. According to [4], the appearance of higher order terms in the series expansion for the mean energy $E(T)$, leads to a curvature in the high temperature range of the elastic constants vs. temperature. Experimentally, the graph has been shown to exhibit a linear portion in this temperature range, which enables us to disconsider the higher order terms of the series. Thus $E(T) = K_B T$, where K_B is the Boltzmann constant, will be a reasonable linear approximation for the energy of the atomic oscillation, allowing the temperature dependence of the elastic constants to be expressed as:

$$C_{ij}(T) = C_{ij}^0 (1 - D_{ij}K_B T) \quad (3)$$

2.1.2. Nonlinearity parameter

The ultrasounds propagating through a solid material can produce a waveform distortion induced by the microstructural properties of the material. This is characterized by the existence of a second harmonic whose amplitude is proportional to the square of the amplitude of the fundamental and to the non-linearity parameter β . The degree of material degradation can be evaluated by measuring the nonlinearity parameter of the ultrasound propagation through the material [5]. In this work, we want to estimate the temperature effect on the nonlinearity

parameter for all crystallographic directions. The nonlinearity parameter has the form [6]:

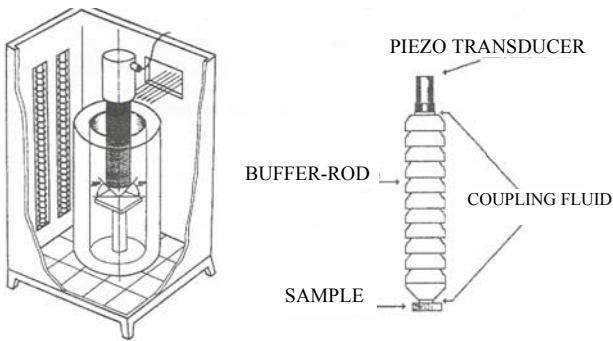
$$\beta = - (3 + K_3/K_2) \quad (4)$$

where K_2 – is a linear combination of the second elastic constants and K_3 – is a linear combination of the third-order elastic constants.

2.2 Modeling

Experiments were made on n-Ge semiconductor samples (sample 1 and sample 2) oriented after the crystallographic axis [111] and [100], respectively. We investigated the variation of the ultrasound attenuation and velocity, under the influence of temperature and frequency which characterize, the mechanical properties of the semiconductor sample material, such as elastic constants C_{ij} , transversal modules G_{111} and G_{100} , the anisotropy factor A and the nonlinearity parameter β . Measurements were made using two successive echoes and for each measurement point, the saved information consists of the amplitude and velocity determined from the reflected RF signal by the USIS program [7]. We used the temperature range from 273 K to 873 K and the frequency domain from 2 MHz to 20 MHz, using Nortec and Krautkramer transducers. Probing at high temperatures was made possible using an Al buffer-rod interposed between the transducer and the sample. The experimental measurements were made using an ultrasonic device Sonic 136 Ultra made by Staveley Corporation.

Buffer-rod. We conceived a practical solution for the fluctuation and non-uniformity of the acoustic pressure across and along the sample in high temperature conditions as well as to maintain and accurately measure a constant temperature along the sample. The oven was provided with an internal ceramic cylinder having the same diameter as the sample. One end of the buffer is inserted into the cylinder that is in contact with the sample, the other end (approx. 65% of its length) being fitted to the ultrasonic transducer. To avoid excessive heating of the transducer, the external end of the buffer is submitted to a uniform air-draft (Fig. 1a). The Al buffer-rod has low acoustic attenuation; eleven grooves were performed all over its lateral surface in order to minimize acoustic losses due to lateral reflections. The buffer has the diameter $\Phi = 25$ mm and the length $l = 81.4$ mm. The ultrasonic energy concentration on the sample is enhanced through the 30° – cut truncated cones profile on the sampling end (Fig. 1b). A chromium- aluminum thermocouple is inserted at the center of the examined sample in an orifice practiced in the ceramic filter shielding the sample. The glycerin was employed to provide the acoustic coupling of the buffer with the sample [11].



a) Oven
b) Buffer-rod
Fig. 1.

3. Results on n-Ge sample

The n-Ge sample (doped with As) has the following parameters: diameter $\Phi = 28.7\text{mm}$, $L_{[111]}=8.10\text{ mm}$, $L_{[100]}=11.60\text{ mm}$, $\rho=5332\text{ Kg/m}^3$, $N=1.5 \times 10^{16}\text{ cm}^{-3}$, resistivity= $5.4\ \Omega\text{cm}$ (sample1);and sample 2 with resistivity = $20\ \Omega\text{cm}$, $N= 7 \times 10^{13}\text{ cm}^{-3}$.

Applying the adiabatic approximation, we obtained the following empirical relations for the elastic constants of n-Ge and these results were corroborated with the theoretical relations issued by Simon [6]:

$$\begin{aligned} C_{11}(T) &= 132.6(1- 96.7E-10 T) \\ C_{12}(T) &= 52.7(1- 600E-10 T) \\ C_{44}(T) &= 64.8(1-127E-10 T) \end{aligned} \quad (5)$$

where 132.6; 52.7 and 64.8 (GPa) are the elastic constant values at 0 K, determined by extrapolation. We can conclude that for the n-Ge sample, one can draw two plots against temperature for the elastic constants: the experimental (Exp) and the adiabatic approximation (T). Fig. 2 for n-Ge sample, (sample 1) shows the plots of elastic constants C_{ij} against temperature made by these two methods mentioned above.

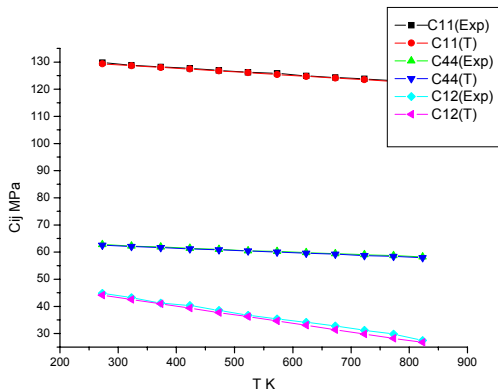


Fig. 2. Temperature plots of the elastic constants for each of the two methods (sample 1).

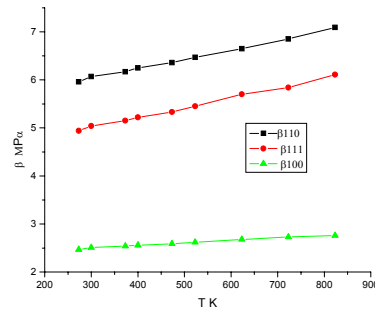


Fig. 3. Dependence of the nonlinearity parameter β on the temperature for the three crystallographic axes.

The analysis of the plot shows that the curves drawn from the experimental determination present the same shape and monotonically decrease with empirical method T, the distinction at C_{12} consisting in the fact that at high temperatures ($\geq 573\text{ K}$) a slight deviation appears between the experiment and theory which disappears at lower temperatures; also at C_{12} it is noticed a faster decrease with the temperature (38.8%) but for the C_{11} the temperature variations are 5.4% and for the C_{44} are 7.3%. With the exception of some slight deviations, we can say there is an identity between the two methods that were found, which proves the validity of the empirical method (T). Therefore, we can conclude there is a linear dependency between velocity and temperature.

By comparing the three elastic constant variations with temperature one can notice a faster decrease for C_{12} after the crystallographic axis [111] and a slower decrease after [100] for C_{11} and C_{44} . These results were expected if we consider the sample as being a system of linear harmonic oscillators [8]. The linear relation between C_{ij} and temperature predicted for high temperatures by the quasiharmonic approximation is close to that observed experimentally. Higher theoretical approximations would be needed to explain the deviation from linearity exhibited by the temperature dependence of $C_{44}=G_{100}$ at high temperatures.

A new confirmation of the validity of the values C_{ij} determined by ultrasounds is the equality from the Keating's relation [9]: $2C_{44}(C_{11} + C_{12}) = (C_{11} - C_{12}).(C_{11} + 3C_{12})$.

4. Discussion

4.1. Nonlinearity parameter, shear modulus, attenuation, buffer-rod

Fig. 3 shows the dependence of the nonlinearity parameter β on the temperature for the three crystallographic axis for n-Ge sample (sample 1). The plots show that the highest values are obtained for the [110] axis. Temperature variations for nonlinearity parameter β are 11% after [100], 16% after [110] and 19% after [111]. We notice a linear, identical and parallel increase for the axis [100] and [111] having the same

variation rate, while for [100] the increase is slower which means that the non-linearity (waveform distortion) is manifesting slower after [100] compared with [111].

4.1.1. Shear modulus

The shears modulus G after the axis [100] and [111] are shown in the plots of Fig. 4.

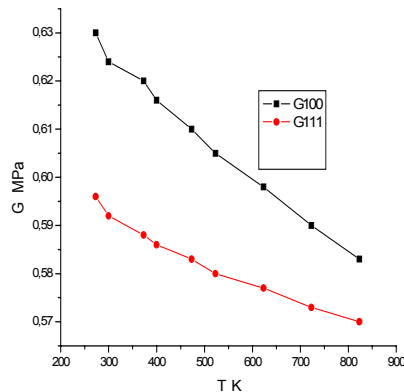


Fig. 4. The shears modulus G .

In this figure, it is noticed a more pronounced decrease for G_{100} . The plots show that the highest values are obtained for the [100] axis. The relative variations of velocity depending on temperature are 7% for the G_{100} and 2% for the G_{111} . Theoretical curve for G_{100} is calculated using the relation $G_{100}(T) = 0.626(1 - 155,4 \cdot 10^{-6} \Delta T)$.

One notices an abrupt decrease after [100] and the decrease becomes linear with the increase of temperature.

Attenuation was another parameter determined experimentally.

4.1.2. Diffraction attenuation

From the experimental determinations made on Ge samples we have obtained attenuation vs frequency due to diffraction for sample 1, and for the sample 2, the graphs are shown in the Fig. 5 in the range 2 MHz - 20MHz.

Analyzing the graph from Fig. 5 one obtain, for the sample 1, the values $A = 3$ and $n = -1.1$ and in this case, the relation for diffraction attenuation is $\alpha_d(f) = 3f^{-1.1}$ and for the sample 2, one obtained the values $A = 2$ and $n = -1.1$ with the relation $\alpha_d(f) = 2f^{-1.1}$.

4.1.3. Intrinsic attenuation

Eliminating the losses by diffraction α_d from the total losses determined experimentally, we have determined the intrinsic attenuation α_{int} which is shown in Figure 6 for the sample1 and sample 2.

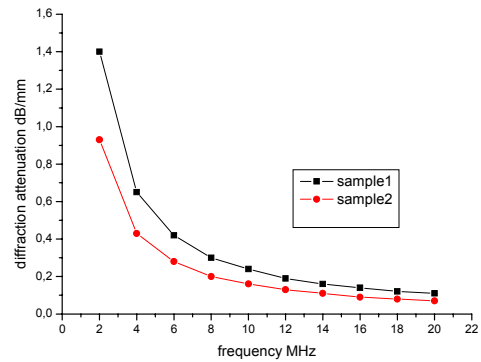


Fig. 5. Diffraction attenuation.

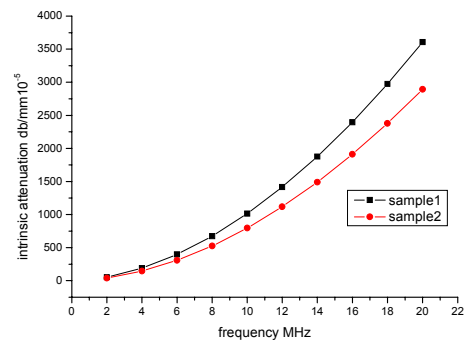


Fig. 6. Intrinsic attenuation.

In the graphs from Fig. 5, we notice that attenuation due to diffraction decreases considerably with the increase of frequency, while at low frequencies, the attenuation is bigger, which is in concordance with the theory that says that at low frequencies, apparent losses prevail.

At sample 1 (n-Ge doped with As), we notice that attenuation values due to diffraction are bigger showing that the doping increases apparent losses. Graphs from Fig. 6 show an intrinsic, «pure» attenuation after eliminating apparent losses. After attenuation coincidence at low frequency values (2-4 MHz), we notice a curves separation towards high frequencies, bigger values having sample 1. The results match Keys' theory [10] which shows that n type materials (arsenic, stibium,phosphorus) doping of Ge significantly increases attenuation.

For the n-Ge sample (sample1) the variation of the intrinsic attenuation depending on frequency has the form $\alpha_{int}(f) = 0.000151f^{1.83}$ and for the sample 2, $\alpha_{int} = 0.0011f^{1.86}$.

4.1.4. Buffer rod

Because the experiments on n-Ge sample were made at high temperatures and we had to use a buffer rod (aluminum), we determined the velocity variation with temperature in this material (buffer rod) which is shown in the graph from Fig. 7. Theoretical curve is calculated using the relation $V_{br}(T) = 6238 - 0.63(T-25)$.

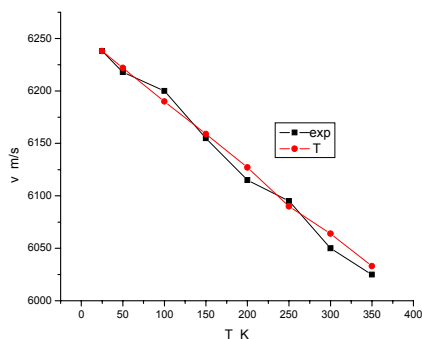


Fig. 7. Velocity vs temperature for B-R.

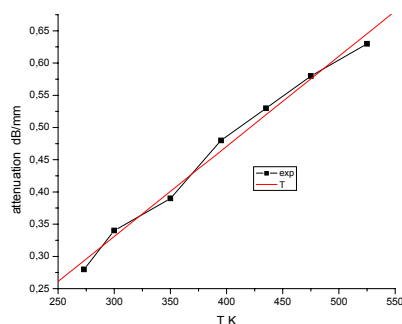


Fig. 8. Attenuation vs temperature for B-R.

The graphs from Fig. 7 show an approximately linear decrease of Al buffer rod velocity with temperature. The empiric relation (T) that was found, corresponds completely with the experimental curve.

Also, for a good knowledge of the influence of the buffer rod on the results, we determined experimentally the attenuation variation with temperature at the buffer rod – n-Ge system. This variation is shown in Fig. 8 along with the theoretical curve calculated with the relation we have found and has the form: $\alpha_{br} = -0.08831 + 0.0014 T$, having an error of 0.0253 and $R^2 = 0.99$.

5. Conclusions

In this paper we determined the acoustic and spectral parameters depending on temperature and frequency. As an experimental set-up we used transducers of different frequencies between 2 MHz and 20 MHz manufactured by Krautkramer and Staveley Corporations and an ultrasonic instrument Sonic 136 Ultra. Regarding elastic constants C_{ij} , we can conclude as it follows: i) the empirical relation (T) given by the author present similar graphics with those obtained by experimental determination; ii) the values of elastic constants determined experimentally prove the validity of the Keating's relation; iii) we have calculated the elastic anisotropy factor and we observed that this factor is constant in the temperature range and is equal to 1.65 ± 0.07 being in good agreement with the one found in literature [8]; iv) the temperature variations for the nonlinearity parameter β are 11% after [100], 16% after [110] and 19% after [111]; v) the temperature variations for the shear modulus are insignificant, namely by the axes [100] is 7% and by [111] is 2%; vi) concerning

the buffer rod influence on measurements, we found an empirical relation of the velocity variation with temperature having the form $V_{br}(T) = 6238 - 0.63(T-25)$ whose curve corresponds with the experimental one; vii) the spectral analysis through the attenuation variation with frequency in the frequency domain is given by a general relation having the form $\alpha(f) = Af^n$, which for the sample 1 has the form $\alpha_d(f) = 3f^{1.1}$ for diffraction attenuation, and $\alpha_d(f) = 2f^{1.1}$ for sample 2 respectively, and for the intrinsic attenuation $\alpha_{int}(f) = 0.00015f^{1.83}$ for the sample 1 and $\alpha_{int} = 0.0011f^{1.86}$ for the sample 2 depending on the range frequency (2 MHz- 20 MHz); viii) the attenuation variation with temperature for the buffer rod-Ge sample is shown in Fig. 10 having the relation $\alpha_{br}(T) = -0.08831 + 0.0014 T$, with an error of 0.0253 and $R^2 = 0.9$.

The differences between the values of the parameters found by us and those from literature are due to the following causes:

- the influence of the nonparallelism of the lateral surfaces on the buffer-rod and on the sample;
- the conversion from the propagation velocity in elastic constants [12];
- multiple reflections occurring as a result of the increase of the ultrasound beam path because of the use of a buffer-rod;
- ultrasound wave velocity $v(f)$ is depending on frequency (dispersion).
- the attenuation coefficient $\alpha(f)$ is depending on frequency and increases with it;
- the velocity and attenuation coefficients are not independent but are tied up with each other and can be determined one from another.

References

- [1] Kyung-Young Ihang, Kyung-Cho Kimm: Ultrasonics **37**, 39(1999).
- [2] R. F. S. Hearmon, Solid State Communications **37**, 915 (1981).
- [3] G. Liebfried, W. Ludwig: Solid State Physics **12**, 45 (1961).
- [4] G. Simon, Journal of Physics Chemistry Solids **28**, 35 (1967).
- [5] D. C. Hurley, D. Balzar: Journal of Applied Physics, **83**, 4584 (1998).
- [6] J. Philip, M. A. Breazeale, Ultrasonics Symposium, 1006 (1980).
- [7] P. Petculescu, R. Ciocan, V. Bokas, Journal of Nondestructive Testing and Ultrasonic **3**, 11 (1998).
- [8] A. Burenkov, S. Nikanorov, A. Stepanov, Soviet Physics-Solid State, **12**, 1940 (1973).
- [9] P. N. Keating, Physical Review **149**, 674 (1966).
- [10] W. P. Mason, Physical Acoustic, Academic Press **III**, B 261 (1965).
- [11] P. Petculescu, J. Matei, J. Optoelectron. Adv. Mater. **6**, 1 (2004).
- [12] P. Petculescu, Insight-British Journal of Nondestructive Testing **12**, 880 (1996).

*Corresponding author: petculescu@univ-ovidius.ro